Axial-vector anomaly in K_L and related decays*

A. Gavrielides
Department of Physics and Astronomy, University of Minnesota, Minneapolis, Minnesota 55455
(Received 25 July 1974)

The $K_L \to 2\gamma$ decay is examined in the context of gauge models of weak and electromagnetic interactions. It is shown that the decay is possible because of the existence of an anomaly in the divergence of the axial-vector current that transforms like λ_6 under SU(3). The existence of such an anomaly is first shown in an SU(2) × U(1) gauge model containing only the familiar quarks, and then generalized and calculated for the realistic case of the SU(4) model of Glashow, Iliopoulos, and Maiani. The $K_L \to 2\gamma$ rate is obtained as a function of the amount of SU(4) breaking, which is determined to be of the order of 1.5 GeV^2. In addition, the $K_L \to \bar{\mu}\mu$ decay is examined within the context of the above models and is shown to be sufficiently suppressed. Moreover, the examination of $K_S \to \pi^+\pi^-$ decay and the $K_L - K_S$ mass difference leads to an interesting relation independent of mass parameters. Also, in the case of the SU(4) model, the calculation of those processes leads to the determination of the quark mass parameters.

I. INTRODUCTION

Several attempts in the past to calculate the $K_L \to 2\gamma$ decay rate using a variety of phenomenological models of weak interactions were met with varying degrees of success. With the advent of gauge theories, however, the possibility of examining the decay within a renormalizable model of weak interactions was made possible. In particular, within the context of such a model and partially conserved axial-vector current (PCAC), the $K_L \to 2\gamma$ decay rate should vanish in the low-energy limit, unless there exists an anomaly to the divergence of the axial-vector equation

$$\partial^\mu J^6_{5\mu} = 2mi J^6_5 . \tag{1}$$

Superscripts refer to the SU(3) transformation properties of the currents.

The purpose here is to examine such a possibility in models of weak interactions, and then explicitly show the existence of the anomaly and its magnitude. Such a calculation would show whether the model has any realistic use whatsoever, if the applied assumptions prevail, and the process would also serve to illustrate several illuminating features of renormalizability of broken gauge field models.

In the following section, two different types of models will be examined: an unrealistic but simple model that contains strangeness-changing neutral currents, and an extension of the Glashow-Iliopoulos-Maiani (GIM) model that contains a charmed quark, i.e., SU(4).[1] It will be shown that in both models an anomaly exists to Eq. (1), and therefore, in the low-energy limit, the $K_L \to 2\gamma$ rate is determined. Such determination allows one to obtain information about the masses of the quarks. In particular, in the SU(4) model, one determines the mass difference between the charmed and uncharmed quarks. If one also looks at $K_L \to \bar{\mu}\mu$, then the absolute magnitude of the mass is determined.

Another model of weak interactions is the one based on $SU(2)_R \times U(1)_L$ symmetry and extended to include color quarks.[2] In this model, one finds that the anomaly is zero, if one assumes that color SU(3) is not broken by mass terms, and here, therefore, the $K_L \to 2\gamma$ decay vanishes in the low-energy limit. Naturally, if color SU(3) is broken, a determination of the amount of breaking can be made this way.

It will be shown in perturbation theory that an anomaly to Eq. (1) exists, whose nature is unique to gauge field models. It arises, essentially, because of the nonminimal type of coupling of the photon to the charged vector-boson current. In particular, if one retains only the convection part of the coupling, no anomaly exists. The part that is responsible for the anomaly then is the left-over magnetic-moment coupling. Such a division of the charged current will be made later in the calculation, and the separate effects will be examined. Since this type of coupling is determined by the non-Abelian nature of the group of weak and electromagnetic interactions, this type of anomaly will exist in most such theories, where the photon couples nonminimally.

In addition, some other interesting processes are examined within the context of those models. The question of the suppression of the $K_L \to \bar{\mu}\mu$ rate is taken, and a calculation shows that a quark mass of a few GeV suffices to give rather good agreement with the available experimental rates. Additional information can be obtained by looking at the $K_S \to \pi^+\pi^-$ rate and also the K_L-K_S mass difference. One obtains results that seem to be

quite encouraging and self-consistent within the approximations that were made. Finally, a rather interesting relation among the above-mentioned processes is obtained in which no quark mass terms appear at all, and which applies equally well for the Gell-Mann–Zweig, Han-Nambu, or colored-quark model, within the context of the $SU(2)_R \times U(1)_L$ model of weak interactions.

II. MODELS

A. The model and Feynman rules

The following model of weak and electromagnetic interactions was adopted for the calculation of the anomaly. The group is $SU(2)_L \times U(1)_R$ under which the following assignments are made:

$$\begin{pmatrix} \mathcal{P} \\ \mathcal{N}' \end{pmatrix}_L \quad \text{and} \quad \lambda'_L$$

are left-handed doublet and singlet, respectively, $\mathcal{P}_R$, $\mathcal{N}_R$, λ_R are singlets, $\vec{A}_\mu$ and B_μ are a triplet and a singlet, respectively, of gauge bosons, and ϕ is a scalar complex doublet. The prime denotes Cabibbo-rotated fields. Then in the familiar way, the following Lagrangian results:

$$\mathfrak{L} = -\tfrac{1}{4}(A'_{\mu\nu})^2 - \tfrac{1}{4}(B_{\mu\nu})^2 + \bar{q}'_L\left(i\partial\!\!\!/ + g\tfrac{1}{2}\vec{\tau}\cdot\vec{A}\!\!\!/ - g'\frac{1}{\sqrt{3}}\frac{\lambda_8}{2}B\!\!\!/\right)q_L + \bar{q}_R\left(i\partial\!\!\!/ - g'\frac{\lambda_Q}{2}B\!\!\!/\right)q_R + |(\partial_\mu - ig\tfrac{1}{2}\vec{\tau}\cdot\vec{A}_\mu + ig'\tfrac{1}{2}B_\mu)\phi|^2$$
$$- \mu^2\phi^2 - h\phi^4 - \mathfrak{L}(\phi, q), \qquad (2)$$

where

$$\vec{A}'_{\mu\nu} = \vec{A}_{\mu\nu} - g\vec{A}_\mu \times \vec{A}_\nu, \quad \vec{A}_{\mu\nu} \equiv \partial_\mu\vec{A}_\nu - \partial_\nu\vec{A}_\mu$$

and $\mathfrak{L}(\phi, q)$ contains the quark-scalar interactions.

Although this model suffers a severe drawback, namely, that it contains neutral strangeness-changing currents, it is very useful for two reasons: It has the advantage of being very simple, containing only the minimum number of fields needed, and it can also be generalized and extended to other models very easily, its results needing only minor modification. Its results on $K_L \to 2\gamma$ can accommodate any model with additional quarks based on $SU(2)_L \times U(1)_R$, such as color or SU(4), and also models based on SO(3) symmetry, such as the Georgi-Glashow model.[3] Of course, it has the disadvantage that one must deal here with strangeness-changing neutral currents in addition to the charged current, but this is a small inconvenience.

Then, one proceeds in the usual way to break the symmetry by giving the neutral scalar member of the doublet a vacuum expectation value. One obtains the familiar fields W^+_μ, W^-_μ, W^0_μ (weak bosons) and A_μ (the electromagnetic field). To zeroth order, one obtains the same relations among the constants as in the Weinberg model.[4] A summary of the propagators and vertices is shown in Fig. 1.

The 't Hooft[5] gauge is used with the following choices:

$$\mathfrak{L}_g = -\xi\left|\partial_\mu W^{+\mu} - \frac{iM_+}{\xi}\phi^+\right|^2 - \frac{\eta}{2}\left(\partial_\mu W^{0\mu} - \frac{M_0}{\eta}x_4\right)^2, \qquad (3)$$

where x_4 is the combination $(i/\sqrt{2})(\phi_0^* - \phi_0)$. In addition, one chooses $\xi = \eta = 1$ so that the vector propagator is in the Feynman gauge. This, then, simplifies the calculations considerably, at the expense of having to consider a larger number of diagrams. This scheme can be understood in terms of a $G_s \times G_w$ over-all scheme, where G_s is the group of strong interactions, as suggested by Weinberg.[6] However, for our purposes here, the nature of G_s can be left unspecified, as long as it does not affect the choice of G_w.

B. Nature of the anomaly

Since K_L transforms like λ_6 under SU(3), one is led to the consideration of $J^6_{5\mu}$, where the superscripts refer to their SU(3) properties. In examining the equation $\partial^\mu J^6_{5\mu} = J^6_5$ in perturbation theory, it is immediately clear that no anomaly can result from the simple triangle to order e^2 since it vanishes. Therefore, one must look at weak radiative corrections to the simple triangle in the next e^2g^2 order. To this order, the formal argument used in the $\pi^0 \to 2\gamma$ case can be applied to see whether the surface terms produced by taking the divergence of the matrix element $\langle 0|J^3_{5\mu}|2\gamma\rangle$ cancel by pairs.[7] It must be pointed out that the argument depends on the assumption that the fermion-loop integration can be performed first, followed by the integration of the radiative-correction loops. One then finds that, by a shift of integration variable, the surface terms cancel. In the case of $\pi^0 \to 2\gamma$ the linear divergence of the surface terms of the basic triangle do not permit this cancellation and give rise to the anomalous term. However, even if one has used this formal argument to imply that higher orders do not contribute to the anomaly, one still has to perform an actual calculation to show that

this is, in fact, what happens. This was done in the $\pi^0 \to 2\gamma$ case to order e^4, and was recently shown by Zee to all orders of e by use of the Callan-Symanzik[8] equation.

If one now uses this formal argument for the matrix element of $\partial^\mu J^6_{5\mu} = 2mi J^6_5$, one can show immediately that it fails because the cancelling surface terms have different weights, essentially because of the fact that the group structure here is of the SU(3) type, and the λ matrices that enter the calculation do not commute. In other words, the propagator that the photons attach to could be a $\mathcal{P}$-quark propagator, in which case the weight is $\frac{4}{9}$, or an $\mathfrak{N}$-quark propagator, in which case the weight is $\frac{1}{9}$. For example, for the subset of the contributing diagrams in which neither of the photons attaches to the charged vector-boson propagator, the resulting sum of surface terms is

$$\sum_{\text{perm. of } i,j,k,m} \mathrm{Tr}([\lambda_6, \lambda_i]\lambda_j\lambda_k\lambda_m)\,\mathrm{Tr}\left(\gamma_5\Gamma_i \frac{1}{\not p + \not k_1 - m}\Gamma_j \frac{1}{\not p + \not k_2 - m}\Gamma_k \frac{1}{\not p + \not k_3 - m}\Gamma_m \frac{1}{\not p + \not k_4 - m}\right), \tag{4}$$

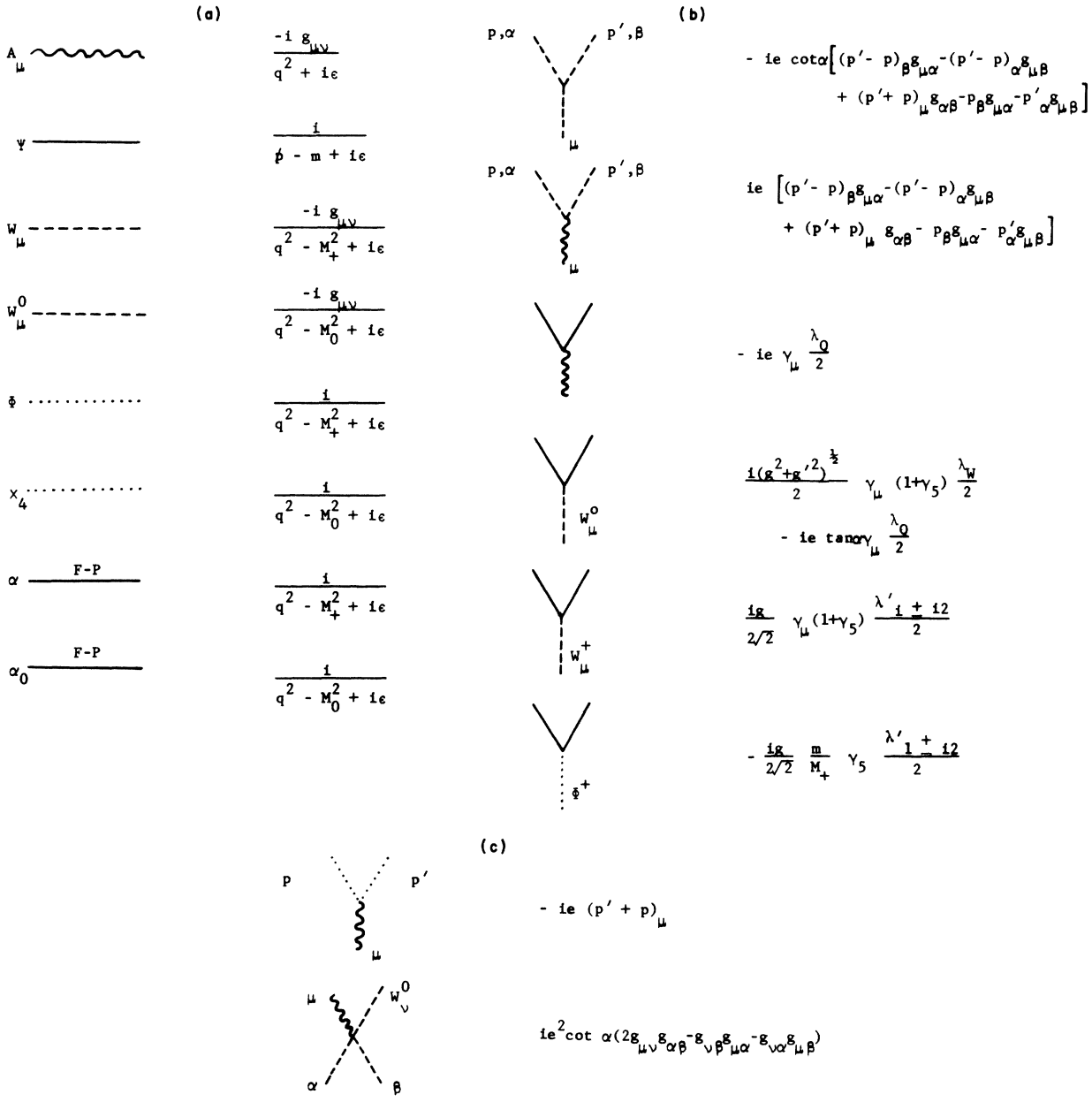

FIG. 1. A small sample of Feynman rules for the model.

with

$$i,j,k,m=(1+i2)',\ (1-i2)',q,q;$$

the notation implying that

$$\lambda_{(1+i2)'}=e^{-i\lambda_7\theta}\lambda_{1+i2}e^{i\lambda_7\theta},$$

$$\Gamma_{(1+i2)'}=\Gamma_{(1-i2)'}=\gamma_\mu(1+\gamma_5),$$

$$\lambda_q=\frac{1}{2}\left(\lambda_3+\frac{1}{\sqrt{3}}\lambda_8\right),\quad \text{charge matrix}$$

$$\Gamma_q=\gamma_\nu .$$

Here then, it is obvious that $\mathrm{Tr}([\lambda_6,\lambda_i]\lambda_j\lambda_k\lambda_m)$ is not equal to zero for all possible permutations, and therefore the surface terms remain.

It is seen here that although no anomaly arises to lowest order, it is, nevertheless, possible for an anomaly to exist in higher orders.

A calculation of the anomaly to order e^2g^2 will now be performed in the following way: Define

$$\langle 0|\partial^\mu J^6_{5\mu}|2\gamma\rangle=(2\omega_1\omega_2)^{1/2}\epsilon_{\mu\nu\alpha\beta}k_1^\alpha k_2^\beta\epsilon_1^\mu\epsilon_2^\nu \times g(k_1,k_2)$$

and

$$\langle 0|2miJ^6_5|2\gamma\rangle=(2\omega_1\omega_2)^{1/2}\epsilon_{\mu\nu\alpha\beta}k_1^\alpha k_2^\beta\epsilon_1^\mu\epsilon_2^\nu \times f(k_1,k_2).$$

In the limit $p^2=(k_1+k_2)^2\to 0$, one can show by use of the Sutherland-Veltman[9] theorem that $g(0,0)=0$. Therefore, if an anomaly exists, the matrix element $\langle 0|2miJ^6_5|2\gamma\rangle$ does not vanish in this limit and

$$A=-\lim_{p^2\to 0}\langle 0|2miJ^6_5|2\gamma\rangle$$

$$=-(2\omega_1\omega_2)^{1/2}\epsilon_{\mu\nu\alpha\beta}k_1^\alpha k_2^\beta\epsilon_1^\mu\epsilon_2^\nu f(0,0).$$

In the calculation, one can separate out the contributions to $f(0,0)$ in terms of sets of diagrams, in which the particles exchanged are vector bosons, scalar ghosts, or scalar particles. Looking at the coupling, one sees that the scalar ghost contribution, when it attaches to fermions, is down by a factor of $(m/M_+)^2$, a number that one can assume to be much smaller than unity. As far as the scalar particle is concerned, the usual procedure is to assume it to be very massive, and so eliminate its effects. Therefore, in the approximation where $(m/M_+)^2\ll 1$ one need look only at diagrams in which both neutral and charged vector bosons contribute.

The possible types of diagrams that enter in the calculation are shown in Figs. 2, 3, and 4. The grouping is according to whether the particle involved in the insertion is neutral or charged. Figure 2 includes all the types of diagrams in which the neutral vector boson enters. Figure 3 includes all types of diagrams in which charged vector bosons contribute. Finally, Fig. 4 shows diagrams in which both neutral and charged vector bosons enter, and their inclusion in either group is not clear.

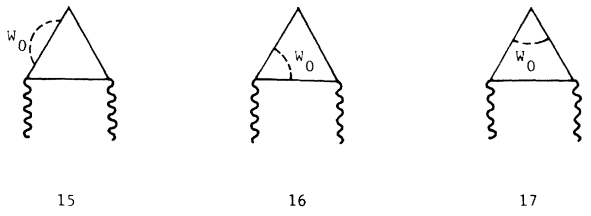

FIG. 2. Neutral-vector-boson contributions to the anomaly.

III. CALCULATION OF THE ANOMALY

A. Calculation of the anomaly and discussion

We begin by examining the graphs appearing in Fig. 2. These graphs involve exchanges of neutral vector bosons only. The current to which W^0_μ cou-

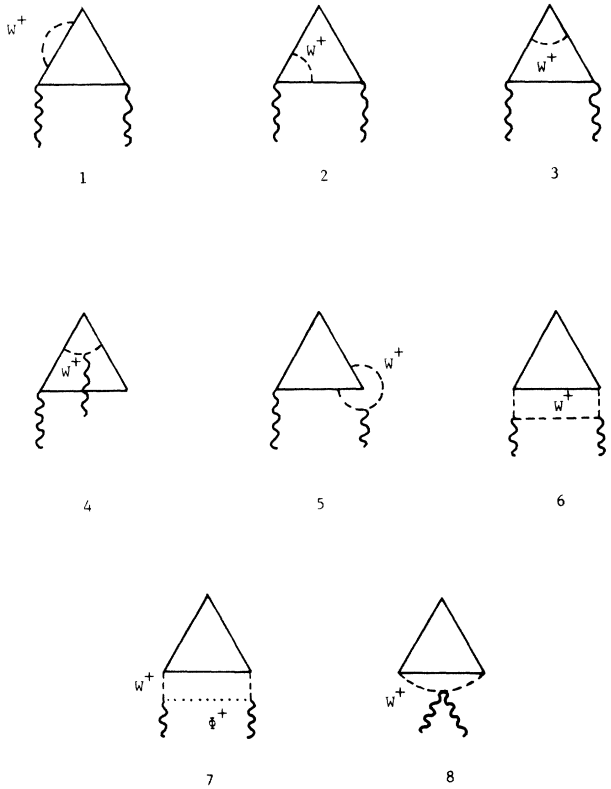

FIG. 3. Charged-vector-boson contributions to the anomaly.

ples is

$$J_\mu^0=\frac{(g^2+g'^2)^{1/2}}{2}\bar{q}\gamma_\mu(1+\gamma_5)\frac{\lambda_W}{2}q-e\tan\alpha\bar{q}\gamma_\mu\frac{\lambda_Q}{2}q.$$

Therefore, one expects two types of contributions: type (a) through the square of the first term of the current proportional to $4e^4/\sin^2 2\alpha$, and type (b) through the cross product of the two terms proportional to $e^4/\cos^2\alpha$, where $\tan\alpha=g'/g$, α being the Weinberg angle. Denoting the contribution of each graph by f_i, i corresponding to the way the graphs are numbered, one can show after some lengthy evaluation of the integrals involved that for each type mentioned

$$f_{15}^{(a)}+f_{16}^{(a)}+f_{17}^{(a)}=0$$

and

$$f_{15}^{(b)}+f_{16}^{(b)}+f_{17}^{(b)}=0.$$

One notes that this is the same type of calculation involved as in the case of the fourth-order corrections to the anomaly in the $\pi^0\to 2\gamma$ case, with the only difference being that the vector particle is massive. Nevertheless, their sum is still equal to zero. Continuing now with contributions from the diagrams in Fig. 3, one can obtain, after some lengthy calculation, the following expression for the contributions of diagrams 1–3 of Fig. 3:

$$f_1+f_2+f_3=-\frac{48h'}{9}\frac{(-1)^{6-n}}{(-m^2)^{4-n}}\frac{\Gamma(5-n)}{\Gamma(4)}\left[\int_0^1 dx\,dy\,x^{3-n/2}(1-x)^{1-n/2}y^{4-n/2}\frac{[(5-n)/(4-\frac{1}{2}n)](6-4x+\frac{1}{4}nx)}{[y+\gamma^2x(1-x)(1-y)]^{6-n}}\right.$$
$$\left.-\tfrac{1}{2}\int_0^1 dx\,dy\,x^{3-n/2}(1-x)^{1-n/2}y^{4-n/2}\frac{[(4-n)/(4-\frac{1}{2}n)](1+x)}{[y+\gamma^2x(1-x)(1-y)]^{5-n}}\right]. \quad (5)$$

where

$$\gamma=M_+/m$$

and

$$h'=e^2g^2\sin\theta\cos\theta\,i^2\pi^n/(2\pi)^{2n}.$$

Note that the calculations are done in the dimensional regularization scheme.[10] As expected, the contribution of this type of graph is not equal to zero, and gives the contribution of the surface terms in Eq. (4). In diagrams 4 and 5 of Fig. 3, one starts to encounter some problems. Their contribution is to be separated into two parts according to the type of vector-boson current they involve. The part which involves the $(p'+p)_\mu g_{\alpha\beta}$ term is the usual convection current, and its contribution will be denoted by f_4^c and f_5^c. The rest of the current involves the magnetic-moment and anomalous-magnetic-moment current of the vector boson, and their contributions will be denoted by f_4^M and f_5^M, respectively. The piece that we are interested in now is the convection-current contribution, denoted by f^c, which sums up to

$$f_4^c+f_5^c=\frac{72h'}{9}\frac{(-1)^{6-n}}{(-m^2)^{4-n}}\frac{\Gamma(5-n)}{\Gamma(4)}\int_0^1 dx\,dy\,x^{3-n/2}(1-x)^{1-n/2}y^{4-n/2}\frac{2-x}{[y+\gamma^2x(1-x)(1-y)]^{6-n}}. \quad (6)$$

Therefore, so far, the sum of diagrams 1–5 of Fig. 3, including only convection currents, is

$$f_1+f_2+f_3+f_4^c+f_5^c=-\frac{48h'}{9}\frac{(-1)^{6-n}}{(-m^2)^{4-n}}\frac{\Gamma(5-n)}{\Gamma(4)}\frac{4-n}{4-\frac{1}{2}n}$$
$$\times\int_0^1 dx\,dy\,x^{3-n/2}(1-x)^{1-n/2}y^{4-n/2}\left[\frac{\frac{7}{2}(1-x)+(\frac{1}{4}nx+1)}{[y+\gamma^2x(1-x)(1-y)]^{6-n}}-\frac{\frac{1}{2}(1+x)}{[y+\gamma^2x(1-x)(1-y)]^{5-n}}\right]$$
$$=0. \quad (7)$$

The reason that the sum vanishes, of course, is that the integrand is finite at $n=4$ and the whole expression is proportional to $(n-4)$. One can dispense easily with diagram 8 of Fig. 3 since it is easy to show that its contribution is zero.

Forgetting for a moment f_4^M and f_5^M, one can look at the contribution of f_6, which is finite. Here, the piece that consists of the convection-convection part of the vector-boson current vanishes and $f_6=f_6^M$.

Therefore, so far, we obtained a remarkable result in that, if one includes only the convection parts of the vector-boson current, the contribution to the anomaly is zero, even though the vector boson is massive. This cancellation, although it was shown for the Gell-Mann–Zweig model, still persists for the colored-quark model. A very similar analysis can be made also for the

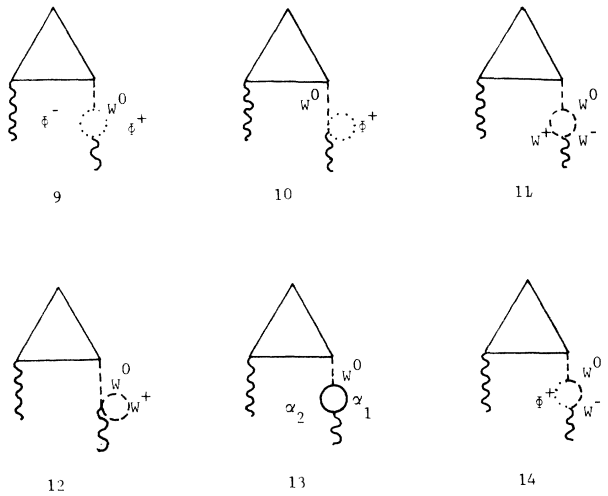

FIG. 4. Feynman diagrams in which both neutral and charged vector bosons contribute to the anomaly.

Han-Nambu model, which shows that the same cancellation exists. All that remains now is to consider f_4^M, f_5^M, f_6^M, and f_7. Here, one clearly encounters a different problem in that f_5^M is logarithmically divergent, but f_4^M, f_6^M, and f_7 are finite. For the theory to be renormalizable, therefore, the divergence of f_5^M must be cancelled against divergences from types of graphs not considered so far. Those could only come from graphs in Fig. 4. Therefore, graphs in Figs. 2 and 4 must be considered together if we are to obtain a finite result for the calculation.

As shown in the Appendix, diagrams 11–14 of Fig. 4 have a logarithmic divergence that cancels that of f_5^M. The grand sum in the limit $M_+^2/m^2 \gg 1$ then contributes to the anomaly

$$A = 96h(\ln\gamma^2 + 3)\,, \tag{8}$$

where

$$h = g^2 e^2 \sin\theta\cos\theta \left(\frac{i}{96\pi^2}\right)^2\,,$$

a result much too large, actually by a factor of 10^2 in the amplitude of $K_L \to 2\gamma$, to be even seriously considered for a moment. The difficulty can be traced back to the contribution of the diagrams in Fig. 4. It is, in fact, solely the terms coming from neutral currents that are proportional to the constant and $\ln\gamma^2$, whereas the diagrams with charged currents contribute leading terms proportional to $1/\gamma^2$ and $(\ln\gamma^2)/\gamma^4$. This is, of course, nothing new since one gets into trouble with strangeness-changing neutral currents by looking at the second-order graph in $K_L \to \bar{\mu}\mu$ decay. However, it is essential to note here that the mass of W_μ^0 does not appear explicitly. Clearly, we have to eliminate neutral strangeness-changing currents and see what we can then obtain. For this purpose, in Sec. III B, we would enlarge the number of basic fields by using one additional quark and moving on to broken SU(4) symmetry of strong interactions.

B. Calculation of the anomaly in the GIM model

The most obvious way to adjust the model so that the neutral strangeness-changing current is absent is to increase the number of quarks by adding a charmed quark, and arranging them in two doublets

$$\begin{pmatrix} \mathcal{P}' \\ \mathfrak{N}' \end{pmatrix}_L \text{ and } \begin{pmatrix} \mathcal{P}' \\ \lambda' \end{pmatrix}_L\,,$$

where $\mathcal{P}'$ has the same quantum numbers as $\mathcal{P}$, except charm. In this way, one arrives at the GIM model which contains only strangeness-conserving neutral currents, since cross terms in the neutral combination $\bar{\mathfrak{N}}'\Gamma\lambda' + \bar{\lambda}'\Gamma\mathfrak{N}'$ cancel.

An interesting modification of this scheme is the model based on color SU(3) where the charmed quark is replaced by $\mathcal{P}_2$, i.e., the structure under $SU(2)_L \times U(1)_R$ is

$$\begin{pmatrix} \mathcal{P}_1 \\ \mathfrak{N}_1' \end{pmatrix}_L\,, \quad \begin{pmatrix} \mathcal{P}_2 \\ \lambda_1' \end{pmatrix}_L$$

and the rest singlets, as recently proposed by Zee.[2] Another model close to this is the three-quartet model based on the $SU(4) \times SU(3)$ group of strong interactions. Here, the structure under $SU(2)_L \times U(1)_R$ is

$$\begin{pmatrix} \mathcal{P}_i \\ \mathfrak{N}_i' \end{pmatrix}_L\,, \quad \begin{pmatrix} \mathcal{P}_i' \\ \lambda_i' \end{pmatrix}_L\,,$$

with $i = 1, 2, 3$ running over color. Both above-mentioned extensions are rather straightforward and will be discussed at the end of this section.

For the GIM model, the calculation of the anomaly now becomes considerably easier. Disregarding all diagrams that contained neutral strangeness-changing currents that were considered previously, one arrives at the set of diagrams shown in Fig. 3, with one important modification.

Owing to the charmed

$$-\bar{\mathcal{P}}'\gamma_\mu(1+\gamma_5)\mathfrak{N} + \bar{\mathcal{P}}'\gamma_\mu(1+\gamma_5)\lambda + \text{H.c.}$$

piece contained in the charged current, for each diagram shown in Fig. 3 that contains a $\mathcal{P}$-quark propagator, there exists an identical diagram in which the $\mathcal{P}$-quark propagator is replaced by a $\mathcal{P}'$-quark propagator, and a relative negative

over-all sign. Therefore, if one calculates the anomaly in the limit of exact SU(4), one finds that there exists no anomaly and K_L does not decay to 2γ. However, since we know that the group of strong interactions is SU(3), one might consider a broken SU(4) group, the breaking being proportional to the mass difference of charmed and uncharmed quarks. This then implies that the $K_L \to 2\gamma$ matrix element is proportional to this mass difference.

Proceeding with the examination of the diagrams in Fig. 3, one finds

$$f_1+f_2+f_3+f_4^c+f_5^c=0\,, \tag{9}$$

where now f_i, the amplitude for the ith type diagram, contains contributions from both the diagram with $\mathcal{P}$ quark and the identical diagram with $\mathcal{P}'$ quark. As before, the superscript c indicates that only contributions from the convection part of the charged current are included.

One point to note also here is that all amplitudes are finite owing to the above-mentioned mechanism and, therefore, there is no need for regularization. Equation (9) shows again the cancellations encountered previously. However, what is more surprising about Eq. (9) is that the sum of the set of diagrams containing only $\mathcal{P}'$ quarks also vanishes in spite of the fact that the propagator of the $\mathcal{P}'$ quark has a different mass than the rest. Again, one is left here with contributions from the magnetic-moment part of the charged current, coming from diagrams 4–7 of Fig. 3. One then finds

$$A=-(f_4^M+f_5^M+f_6+f_7)$$
$$\simeq \frac{\sqrt{2}\,G\alpha}{3\pi^3}\sin\theta\cos\theta\,\frac{\Delta m^2}{m_N^{\,2}} \tag{10}$$

in the approximation $\gamma^2 \gg 1$, $(m_{\mathcal{P}'}{}^2/m_{\mathcal{P}}{}^2)-1<1$, where $\gamma=M_+/m$ as before, $\Delta m^2=m_{\mathcal{P}'}{}^2-m_{\mathcal{P}}{}^2$, and $G=10^{-5}$. The exact expression is given in Appendix B.

Using the experimental value of $K_L \to 2\gamma$, one then obtains $\Delta m^2/m_N{}^2=1.5$, a small number, but within the realm of possibility.

For the three-quartet model, this number represents the amount of SU(4) breaking. In the case of the colored-quark model mentioned at the beginning of this subsection, $\Delta m^2/m_N{}^2=1.5$ gives the breaking in color SU(3).

Additional information can be obtained if one now looks at $K_L \to \bar{\mu}\mu$ within the models discussed so far. Results to be discussed later indicate that $m^2 \leq 5$ GeV^2 gives enough suppression to the diagram with a $2W$ intermediate state.

It seems that the most promising models of weak interaction, those based on $SU(2)_L \times U(1)_R$ colored or otherwise, are within the realm of possibility as far as results from this analysis indicate.

IV. CALCULATION OF THE $K_L \to \bar{\mu}\mu$ RATE

The $K_L \to \bar{\mu}\mu$ process is of considerable interest because, experimentally, the rate is suppressed to a great degree. In part, this argues against the existence of neutral strangeness-changing currents, because the rate seems to be of the order $G^2\alpha^4$ rather than G^2, as would be expected if neutral strangeness-changing currents existed. However, even their absence does not guarantee that the $K_L \to \bar{\mu}\mu$ rate calculated to the second order in perturbation theory would be suppressed enough. That is, the contribution to the amplitude of the effective neutral current, arising by the exchange of two charged vector bosons, could be either of order G^2m^4 or $G\alpha m^2$, where m is the quark mass. In the former case, agreement might be obtained. In the latter case, some additional mechanism of suppression must be evoked. It is therefore advisable that the question be examined in perturbation theory within the context of gauge theories. It is also of interest to note that the $K_L \to \bar{\mu}\mu$ rate is very close to the unitarity bound, as computed from the 2γ intermediate state. Therefore, even though the contributions of the diagrams shown in Fig. 5 happen to be of the order G^2, it still could be difficult to obtain agreement.

The calculation is done here for the SU(4) case of strong interactions, with the $\mathcal{P}'$ mass larger than the mass of the SU(3) triplet. As discussed previously, calculations in this model can be easily adjusted to yield results for the other quark models discussed previously. The calculation of the fourth-order diagrams in Fig. 5 is straightforward, but rather lengthy. A few of the steps and relevant details are summarized in Appendix C. Here, we quote only the final result for the sum of contributions of the diagrams shown in Fig. 5.

Let this amplitude be $A^W(K_L \to \bar{\mu}\mu)$, the W indicating that diagrams with W exchanges only enter. This amplitude is then given by

$$A^W(K_L \to \bar{\mu}\mu)=\frac{3iG^2}{32\pi^4}\,\frac{m^2 m_\mu \Delta m^2}{f_K m_N{}^4}\cos\theta\sin\theta\ln\gamma^2\,\bar{u}\gamma_5 v\,. \tag{11}$$

This is in the approximation $\gamma^2 \gg 1$, $(\alpha^2-1)<1$, where $\gamma^2 \equiv M_+{}^2/m^2$ and $\alpha^2 \equiv m_{\mathcal{P}'}{}^2/m_{\mathcal{P}}{}^2$.

A note of caution must be inserted here. Equation (11) has an explicit dependence on the quark mass. It is not, therefore, as reliable as expressions obtained from quark-loop calculations that turn out to be mass-independent.

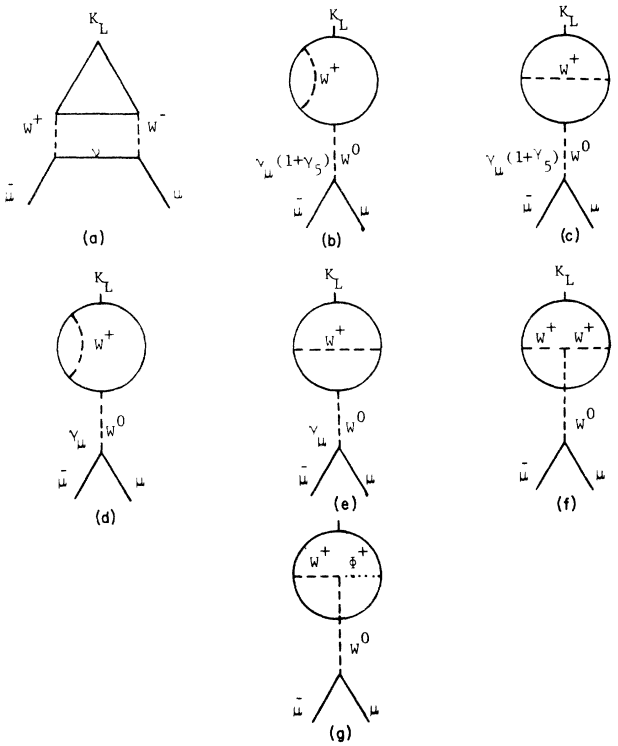

FIG. 5. Feynman diagrams contributing to $K_L \to \bar{\mu}\mu$.

From previous estimates, it is known that $\Gamma(K_L \to \bar{\mu}\mu)_{\text{abs}} = 7.6\times10^{-23}$ MeV, as obtained from the 2γ intermediate state. However, the total experimental rate of $K_L \to \bar{\mu}\mu$ is presently uncertain. Of the two available, the one by the Berkeley group gives an upper limit of $\Gamma(K_L \to \bar{\mu}\mu) < 2.4\times10^{-23}$ MeV. The other, by the BNL-Columbia-NYU group, gives an upper limit of $\Gamma(K_L \to \bar{\mu}\mu) < 13\times10^{-23}$ MeV.[11] We shall use the larger one, since the smaller one is below the unitarity bound.[12] Estimates of the real part of the $K_L \to \bar{\mu}\mu$ that proceeds through the 2γ intermediate state are obtained either by using the dispersion-theory approach or by calculating the diagram shown in Fig. 6 with the $K_L \to 2\gamma$ vertex obtained in the previous analysis and the quark mass as the cutoff. Both results give an estimate of

$$\frac{\mathrm{Re}A^{2\gamma}(\bar{\mu}\mu)}{\mathrm{Im}A^{2\gamma}(\bar{\mu}\mu)} = \frac{2}{3}\,.$$

Thus, we obtain an experimental upper limit on $\Gamma^W(K_L \to \bar{\mu}\mu)$ as follows:

$$\Gamma^W(K_L \to \bar{\mu}\mu) = 3.1\times10^{-7}\,\Gamma(K_L \to 2\gamma)\,. \tag{12}$$

Equation (11) will be compared with this limit later in Eq. (15), along with calculated rates on $K_S \to \pi^+\pi^-$ and $m_{K_L}{}^2 - m_{K_S}{}^2$ to place upper limits on

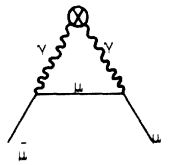

FIG. 6. Feynman diagram for the 2γ intermediate state, in $K_L \to \bar{\mu}\mu$. The vertex is taken to be $V_{\alpha\beta} = c_{\mu\nu\alpha\beta}k_1^\mu k_2^\nu$.

$(m^2/m_N{}^2)\ln\gamma^2$ and independently on $\ln\gamma^2$. However, before we do that, we need to obtain results for the above-mentioned process.

V. THE $K_S \to \pi^+\pi^-$ RATE AND K_L-K_S MASS DIFFERENCE

In addition to $K_L \to \bar{\mu}\mu$ examined previously, the decay $K_S \to \pi^+\pi^-$ and also the K_L-K_S mass difference could contain some more information on the parameters of the model. That is, we should be able to obtain some insight into the magnitude of the quark-mass parameter by considering the above-mentioned processes. Their calculation is readily available in perturbation theory, within the context of gauge theories, by imposing PCAC at the external vertices. We will continue to work with the SU(4) quark model, as we have done most of the time until now.

The diagrams, a total of four, contributing to $K_S \to \pi^+\pi^-$ are given in Fig. 7. Out of those diagrams, (b) and (d) are identically zero, essentially because of the trace on the internal group. The contribution of (a) is smaller than the rest by a factor of $m_K{}^2/M_+{}^2$, and it will be neglected. Therefore, the dominant contribution is that of diagram (c), which turns out to be, in the limit $\gamma^2 \gg 1$,

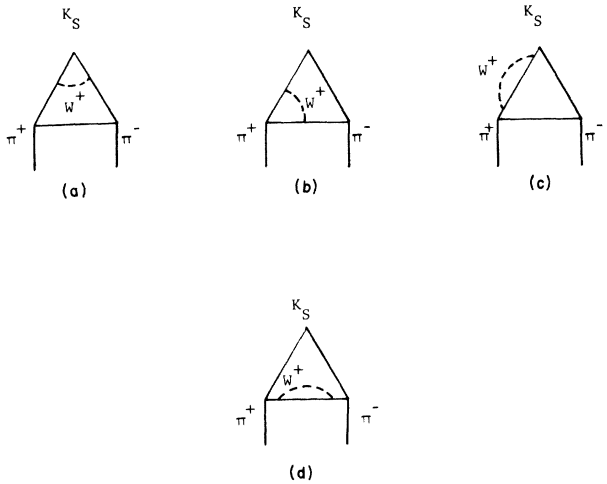

FIG. 7. Feynman diagrams contributing to $K_S \to \pi^+\pi^-$.

$(\alpha^2-1)<1$,

$$A(K_S\to\pi^+\pi^-)=-\frac{G}{\sqrt{2}}\,\frac{\cos\theta\sin\theta}{48\pi^4}\,\frac{m^2\Delta m^2 m_K{}^2}{f_\pi{}^2 f_K m_N{}^2}\,. \tag{13}$$

A calculation of $K_S\to\pi^0\pi^0$ can also be performed along similar lines. Then one obtains the familiar isospin rule

$$\frac{A(K_S\to\pi^+\pi^-)}{A(K_S\to\pi^0\pi^0)}=\frac{1}{\sqrt{2}}\,.$$

Of course, one cannot obtain the $K^+\to\pi^+\pi^0$ rate in this way because to order G^2 it vanishes from purely group considerations. One would have to include electromagnetic corrections in addition, i.e., to order Ge^2 in order to obtain a nonvanishing result. However, at the present time, we will not address ourselves to this problem, although it is not without significance.

Next, we turn to the K_L-K_S mass difference. The pertinent Feynman diagrams are shown in Fig. 8. Here, for diagram 8(a), we observe that the loop integration is being cut off by the mass of the quark, and since both $\mathcal{P}$ and $\mathcal{P}'$ contribute in the intermediate states, the integrations are highly convergent. The vertex shown in Fig. 9 is then calculated, its dependence on the loop momentum in the denominator is dropped, and one obtains for the vertex insertion

$$I_1=\frac{g^2 m}{2M_+{}^2}\,\frac{\pi^2}{(2\pi)^4}\,(\ln\gamma^2-1)(1-\gamma_5)\not{p}\,,$$

p being the external momentum. Then, this vertex is inserted in diagram 8(a) and the resulting contribution to the mass difference is

$$\Delta m_K{}^2(\mathrm{a})=\frac{2G^2}{(2\pi)^6}\,\frac{\Delta m^2 m_K{}^2 m^2}{3m_N{}^4 f_K{}^2}\cos^2\theta\sin^2\theta(\ln\gamma^2-1),$$

where by $\Delta m_K{}^2$ we mean $m_{K_L}{}^2-m_{K_S}{}^2$.

For diagram 8(b), again the self-energy is finite,

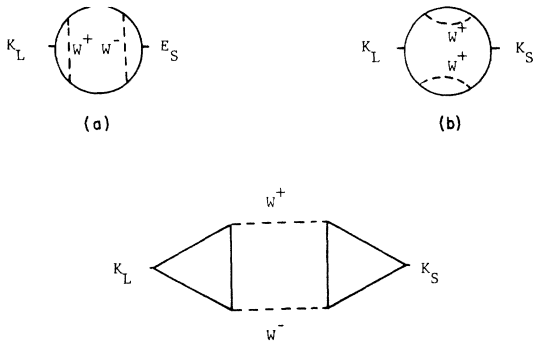

FIG. 8. Feynman diagram for the K_L-K_S mass difference.

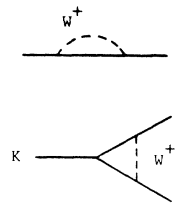

FIG. 9. Self-energy and vertex insertions.

its calculation giving

$$I_2=\frac{g^2\Delta m^2}{4M_+{}^2}\,\frac{i\pi^2}{(2\pi)^4}\,(\not{l}-\not{p})\,.$$

This then inserted in the diagram gives

$$\Delta m_K{}^2(\mathrm{b})=\frac{2G^2}{(2\pi)^6}\,\frac{(\Delta m^2)^2 m^2 m_K{}^2}{12m_N{}^4 f_K{}^2}\cos^2\theta\sin^2\theta\,.$$

Diagram 8(c) and also the one with the crossed boson propagators is more complicated. However, with $\gamma^2\gg1$, one can easily obtain the following result:

$$\Delta m_K{}^2(\mathrm{c})=\frac{16G^2m^2}{(2\pi)^6}\cos^2\theta\sin^2\theta\,\frac{m_K{}^2(\Delta m^2)^2}{f_K{}^2 m_N{}^4}\,L\,,$$

where

$$L=\int_0^1 x^3(1-x)^2\,dx\times\int_0^1 y^3(1-y)^2\,dy\times\int_0^1 v(1-v)\,dv\,\frac{1}{vy(1-y)+(1-v)x(1-x)}\,.$$

An upper limit can easily be placed on L, which results in

$$\Delta m_K{}^2(\mathrm{c})\le\tfrac{4}{565}\,\Delta m_K{}^2(\mathrm{b})\,.$$

Therefore, the contribution of diagram 8(c) can be neglected. Thus, one obtains for the K_L-K_S mass difference

$$\Delta m_K{}^2=\frac{2G^2}{(2\pi)^6}\,\frac{(\Delta m^2)^2 m^2 m_K{}^2}{3f_K{}^2 m_N{}^4}\times\cos^2\theta\sin^2\theta\left[\tfrac{1}{4}+(\ln\gamma^2-1)^2\right]. \tag{14}$$

We will now turn to a discussion of the results obtained so far.

VI. DISCUSSION

In the opening section of this paper, it was seen that we were able to obtain a limit on the magnitude of Δm^2, the squared mass difference between charmed and uncharmed quarks, from an analysis of the $K_L\to2\gamma$ amplitude. Now, we have available

three more expressions, the $K_L \to \bar{\mu}\mu$ rate, the $K_S \to \pi^+\pi^-$ rate, and the mass difference K_L-K_S. All involve, as given by Eqs. (12)–(14), m^2, Δm^2, and $\ln\gamma^2$ in some way or other. Since the numerical value of quark masses depends on the particular quark model that one would choose, be it SU(4), SU(3)$\times$ SU(3), or color SU(3), we can either enumerate those values for each model or obtain expressions that do not involve either m^2 or Δm^2. We have chosen to do the latter, and also to present some of the results for SU(4).

First, we obtain some limits on the functions $(m^2/m_N{}^2)\ln\gamma^2$ and separately on $\ln\gamma^2$ by the use of the calculated rates. From the experimental ratio of $\Gamma^W(K_L \to \bar{\mu}\mu)/\Gamma(K_L \to 2\gamma)$, we can obtain a limit on $(m^2/m_N{}^2)\ln\gamma^2$.

Using Eqs. (11) and (12) we obtain

$$\frac{\Gamma^W(K_L \to \bar{\mu}\mu)}{\Gamma(K_L \to 2\gamma)} = \left| \frac{9G}{16\pi\alpha} \frac{m^2}{m_N{}^2} \right|^2 \frac{m_\mu{}^2}{m_K{}^2} \ln^2\gamma^2 \leq 3.1\times 10^{-7}. \tag{15}$$

This then gives the upper limit

$$\frac{m^2}{m_N{}^2} \ln\gamma^2 \leq 11.5. \tag{16}$$

Similarly, from the experimental ratio $\Gamma^W(K_L \to \bar{\mu}\mu)/\Gamma(K_S \to \pi^+\pi^-)$, we obtain a limit on $\ln\gamma^2$ by

$$\frac{\Gamma^W(K_L \to \bar{\mu}\mu)}{\Gamma(K_S \to \pi^+\pi^-)} = \left| 9G \frac{f_\pi{}^2}{m_N{}^2} \frac{m_\mu}{m_K} \right|^2 \frac{\ln^2\gamma^2}{(1-4m_\pi{}^2/m_K{}^2)^{1/2}} \leq 4\times 10^{-13}, \tag{17}$$

which gives the upper limit

$$\ln\gamma^2 \leq 3.1. \tag{18}$$

To obtain an idea of the magnitude involved, we solve Eqs. (18) and (16) for the upper limit and also use the value $\Delta m^2 = 1.5$ that was determined from the $K_L \to 2\gamma$ rate:

$$\frac{m^2}{m_N{}^2} = 4.1, \quad \frac{m'^2}{m_N{}^2} = 5.6. \tag{19}$$

Unfortunately, those upper limits give a mass for $M_+ = 14$ GeV, a number too low to be acceptable.

However, another determination of m^2 can be made independently by evoking the experimental ratio of $\Gamma(K_S \to \pi^+\pi^-)/\Gamma(K_L \to 2\gamma)$. For this we obtain

$$\frac{\Gamma(K_S \to \pi^+\pi^-)}{\Gamma(K_L \to 2\gamma)} = \left| \frac{1}{16\pi\alpha} \frac{m_N{}^2}{f_\pi{}^2} \right|^2 \left(\frac{m^2}{m_N{}^2}\right)^2 \left(1 - \frac{4m_\pi{}^2}{m_K{}^2}\right)^{1/2} = 7.6\times 10^5. \tag{20}$$

This then gives $m^2/m_N{}^2 = 3.70$, in close agreement with that in Eq. (19).

Now we turn to an interesting equation that we can obtain that is independent of quark mass. Among the rates $\Gamma(K_L \to 2\gamma)$ and $\Gamma(K_S \to \pi^+\pi^-)$ and the K_L-K_S mass difference, we can eliminate all mass dependence except for the function $F = \frac{1}{4} + (\ln\gamma^2 - 1)^2$ that appears in $\Delta m_K{}^2$. That is,

$$\frac{\Delta m_K}{[\Gamma(K_L \to 2\gamma)\Gamma(K_S \to \pi^+\pi^-)]^{1/2}} = \frac{(2\pi)^2}{\alpha} 6F \frac{f_\pi{}^2}{m_K{}^2}. \tag{21}$$

However, it is easy to see that Eq. (18), which gives the upper limit on $\ln\gamma^2$, is not model-dependent. Then imposing this on F, one obtains

$$\frac{\Delta m_K}{[\Gamma(K_L \to 2\gamma)\Gamma(K_S \to \pi^+\pi^-)]^{1/2}} \leq (2\pi)^2 \frac{f_\pi{}^2}{m_K{}^2} \left(\frac{24}{\alpha}\right). \tag{22}$$

It is interesting to note that no weak-coupling constant appears on the right-hand side. It is of further interest, therefore, to speculate whether it is possible for such a relation to be obtained by more general arguments. Also note that the upper limit of this equation is satisfied within a factor of six.

In conclusion, we have examined two models of weak and electromagnetic interactions within the framework of gauge theories. The first model considered contained strangeness-changing neutral currents, and it was used more for theoretical calculations than for its realization in nature.

In the second model, neutral strangeness-changing currents were absent, and its results were taken at face value. We have shown that an anomaly exists in the divergence of the axial-vector current that transforms like λ_6 under SU(3) in both models. This anomaly was explicitly calculated and we also obtained from it the $K_L \to 2\gamma$ rate. The question then of the suppression of the rate $K_L \to \bar{\mu}\mu$ was discussed, and it was shown that within those models we obtained quite satisfactory results, if the quark masses were restricted to some quite reasonable levels. In the process, we were able to obtain also quite reasonable results for the $K_S \to \pi^+\pi^-$ rates and also the K_L-K_S mass difference. The results quoted in Eq. (19) are true only for the SU(4) model, and further, only for the upper limit of Eqs. (18) and (19). For other models, such as SU(3)$\times$SU(3) or color SU(3), the calculated results would have to be adjusted by the relevant factors. Equation (22), which relates the $\Gamma(K_L \to 2\gamma)$ and $\Gamma(K_S \to \pi^+\pi^-)$ to the K_L-K_S mass difference, is model-independent, and its upper limit is satisfied within a factor of six.

ACKNOWLEDGMENT

The author is indebted to Professor H. Suura for help, encouragement, and guidance in this work.

APPENDIX A

In graphs 9 and 10 of Fig. 4, it is easy to see that because of gauge invariance in the limit $p^2 \to 0$, their contribution is zero. Diagrams 11–14 of Fig. 4 give

$$f_{11}+f_{12}+f_{13}+f_{14} = -96h\Gamma(2-\tfrac{1}{2}n) - 96h\left[\frac{\partial\Gamma(z)}{\partial z}\bigg|_{z=1} + \ln(-M_+^2) + \ln(-m^2)\right], \tag{A1}$$

which clearly shows the logarithmic divergences. The contribution of diagrams 11, 12, and 13 of Fig. 4 is proportional to $\cot\alpha$. That of diagram 14 of Fig. 4 is proportional to $\tan\alpha$, so, in that sense, diagram 14 of Fig. 4 fixes things up so that in the end the sum is of the right order. Now we must look at f_5^M. This gives

$$f_5^M = 96h\Gamma(2-\tfrac{1}{2}n) + 96h\left[1 + 2\frac{\partial\Gamma(z)}{\partial z}\bigg|_{z=1} + 2\ln(-m^2)\right] - 192h\int_0^1 \ln x\,dx \int_0^1 y(1-y)\frac{\partial}{\partial x}\left(\frac{(1-x)^2}{y+\gamma^2 x(1-x)(1-y)}\right)dy$$
$$- 144h\int_0^1 x^2\,dx\int_0^1 (1-y)^2\frac{1}{y+\gamma^2 x(1-x)(1-y)}\,dy, \tag{A2}$$

so that the sum of Eqs. (A1) and (A2) is finite and equal to

$$f_{11}+f_{12}+f_{13}+f_{14}+f_5^M = 96h\left[1+\frac{\partial\Gamma(z)}{\partial z}\bigg|_{z=1} - \ln\gamma^2\right] - 192h\int_0^1 \ln x\,dx\int_0^1 y(1-y)\frac{\partial}{\partial x}\left(\frac{(1-x)^2}{y+\gamma^2 x(1-x)(1-y)}\right)dy$$
$$- 144h\int_0^1 x^2\,dx\int_0^1 (1-y)^2\frac{1}{y+\gamma^2 x(1-x)(1-y)}\,dy. \tag{A3}$$

Finally, we are left with finite contributions all together. All that remains is to obtain the contributions from f_4^M, f_6, and f_7 and add those to Eq. (A3). The grand sum of all of them then is

$$f_T = 96h\left[1+\frac{\partial\Gamma(z)}{\partial z}\bigg|_{z=1} - \ln\gamma^2\right] - 192h\int_0^1 \ln x\,dx\int_0^1 y(1-y)\frac{\partial}{\partial x}\left(\frac{(1-x)^2}{y+\gamma^2 x(1-x)(1-y)}\right)dy$$
$$+ 24h\int_0^1 x\,dx\int_0^1 (1-y)\frac{3x(1-y)(8-y)-12x(1-y)-8y}{y+\gamma^2 x(1-x)(1-y)}\,dy$$
$$+ 48h\gamma^2\int_0^1 x^3(1-x)\,dx\int_0^1 (1-y)^3\frac{1}{[y+\gamma^2 x(1-x)(1-y)]^2}\,dy. \tag{A4}$$

For

$$\gamma^2 = M_+^2/m^2 \gg 1,$$

the leading term for the anomaly is

$$A = 96h(\ln\gamma^2 + 3). \tag{A5}$$

APPENDIX B

The complete expression of the anomaly for the case of the GIM model is

$$A = -24h(\alpha^2-1)\int_0^1 x\,dx\int_0^1 (1-y)\,dy\frac{\{12x(1-y)-3(1-y)xy-8[1-x/(1-x)]\}(1-x)y}{[y+\gamma^2 x(1-x)(1-y)][xy+\alpha^2(1-x)y+\gamma^2 x(1-x)(1-y)]}$$
$$- 48h\gamma^2\int_0^1 x^3(1-x)\,dx\int_0^1 (1-y)\,dy\left[\frac{1}{[y+\gamma^2 x(1-x)(1-y)]^2} - \frac{1}{[xy+\alpha^2(1-x)y+\gamma^2 x(1-x)(1-y)]^2}\right].$$

The leading term for $M_+/m \gg 1$ is given by Eq. (10).

APPENDIX C

Here we list some of the calculations for the diagrams of Fig. 5 that lead to the result quoted in Eq. (11). The calculation of diagram (a) is straightforward and leads to

$$A_a = \frac{iG^2}{4\pi^4}\frac{m^2 m_\mu \Delta m^2}{f_K m_N^4}\bar{u}\gamma_5 v\,\frac{\gamma^2}{\alpha^2-1}\int_0^1 x^2\,dx\int_0^1 (1-y)\,dy\int_1^{x+\alpha^2(1-x)} d\lambda\,\frac{1}{[\lambda y+\gamma^2 x(1-x)(1-y)]^2}$$
$$= \tfrac{1}{4}\epsilon\Phi_2\,\bar{u}\gamma_5 v, \tag{C1}$$

with

$$\gamma^2 = \frac{M_+^2}{m^2}, \quad \alpha^2 = \frac{m_{\Phi'}^2}{m_\Phi^2}.$$

For diagrams (b)–(e), in Fig. 5, the coupling of W_μ^0 has been separated into weak coupling [graphs (b), (c)], and the leftover vector coupling proportional to $e\tan\alpha$ [graphs (d), (e)]. One finds with

$$\epsilon = \frac{iG^2}{4\pi^4}\frac{m^2 m_\mu \Delta m^2}{f_K m_N^4}$$

that

$$A_b = -\tfrac{1}{8}\epsilon\bar{u}\gamma_5 v\Phi \tag{C2}$$

and

$$A_c = -(\tfrac{1}{32}\epsilon\Phi + \tfrac{1}{8}\epsilon\Phi_1)\bar{u}\gamma_5 v, \tag{C3}$$

where the parametric integration functions are

$$\Phi = \frac{\gamma^2}{(\alpha^2-1)}\int_0^1 \frac{x}{(1-x)}dx\int_0^1 y^2\,dy\int_1^{x+\alpha^2(1-x)} d\lambda\,\frac{\lambda}{[\lambda y+\gamma^2 x(1-x)(1-y)]^2} \tag{C4}$$

and

$$\Phi_1 = \frac{\gamma^2}{(\alpha^2-1)}\int_0^1 \frac{dx}{(1-x)}\int_0^1 y^2\,dy\int_1^{x+\alpha^2(1-x)} \frac{d\lambda}{\lambda y+\gamma^2 x(1-x)(1-y)}. \tag{C5}$$

Now, proceeding to diagrams (d), (e), (f), and (g) in Fig. 5, we find that the Weinberg angle α enters in the coupling, but in a very particular way. For diagrams (d) and (e), one obtains

$$A_d = \tfrac{1}{24}\epsilon\sin^2\alpha\,\Phi\bar{u}\gamma_5 v, \tag{C6}$$

$$A_e = \tfrac{1}{12}\epsilon\sin^2\alpha\,\Phi\bar{u}\gamma_5 v, \tag{C7}$$

where the function Φ is given in (C4).

Now, in an analogous way to the photon coupling, if one separates the contribution of diagram (f) into the convection and magnetic-moment part due to the coupling of W_0^μ to the charged current as was done in the $K_L \to 2\gamma$, one obtains

$$A_f^c = \tfrac{1}{8}\epsilon\cos^2\alpha\,\Phi\bar{u}\gamma_5 v. \tag{C8}$$

Then, the partial sum of (C6) through (C8) is independent of the angle,

$$A_d + A_e + A_f^c = \tfrac{1}{8}\epsilon\Phi\bar{u}\gamma_5 v. \tag{C9}$$

One then is left with the magnetic-moment (MM) part of diagram (f) and also diagram (g), which give, respectively,

$$A_f^{MM} = \tfrac{1}{4}\epsilon\cos^2\alpha\,\Phi\bar{u}\gamma_5 v \tag{C10}$$

and

$$A_g = \tfrac{1}{4}\epsilon\sin^2\alpha\,\Phi\bar{u}\gamma_5 v, \tag{C11}$$

and again the sum of the contributions of (C4) and (C5) is independent of the angle.

Finally, the total sum gives

$$A^W(K_L \to \bar{\mu}\mu) = \tfrac{1}{32}\epsilon(7\Phi - 4\Phi_1 + 8\Phi_2)\bar{u}\gamma_5 v,$$

which in the approximation $\gamma^2 \gg 1$ yields the result quoted in Eq. (11).

*Work supported in part by the U. S. Atomic Energy Commission under Contract No. AT(11-1) 1764.

[1]S. Glashow, J. Iliopoulos, and L. Maiani, Phys. Rev. D 2, 1285 (1970).
[2]M. A. B. Bég and A. Zee, Phys. Rev. Lett. 30, 675 (1973); Phys. Rev. D 8, 1460 (1973).
[3]H. Georgi and S. L. Glashow, Phys. Rev. Lett. 28, 1494 (1972).
[4]S. Weinberg, Phys. Rev. Lett. 19, 1264 (1967).
[5]G. 't Hooft, Nucl. Phys. B35, 167 (1971).
[6]S. Weinberg, Phys. Rev. Lett. 31, 494 (1973).
[7]S. L. Adler, Phys. Rev. 177, 2426 (1969); S. L. Adler and W. A. Bardeen, *ibid.* 182, 1517 (1969); R. Jackiw and K. Johnson, *ibid.* 182, 1459 (1969).
[8]A. Zee, Phys. Rev. Lett. 29, 1198 (1972).
[9]D. G. Sutherland, Nucl. Phys. B2, 433 (1967); M. Veltman, Proc. R. Soc. A301, 107 (1967).
[10]G. 't Hooft, Nucl. Phys. B33, 173 (1971).
[11]P. Darriulat *et al.*, Phys. Lett. 33B, 249 (1970).
[12]More recent measurements reported by W. C. Carithers *et al.* [Phys. Rev. Lett. 30, 1336 (1973)] and W. C. Carithers *et al.* [*ibid.* 31, 1025 (1973)] give an averaged branching ratio of $\Gamma(K_L \to \bar{\mu}\mu)/\Gamma(K_L \to \text{all}) = (12^{+8}_{-4})\times 10^{-9}$. The use of this new result does not alter the conclusions arrived at in this paper.